WORLD JOURNAL OF PHARMACEUTICAL RESEARCH
Coden USA: WJPRAP Impact Factor 8.63
Volume 15, Issue 17, 680-701. Research Article ISSN 2277–7105

DESIGN SYNTHESIS AND EVALUATION OF IMIDAZOLE [4,5 -B] PYRIDINE BENZO-HYDRAZONE

[*1]Nashra Sami, [2]Purnima Ansari

[*1]Aryakul College of Pharmacy & Research, Lucknow.

[2]Associate Professor, Jahangirabad Institute of Technology, Faculty of Pharmacy, Jahangirabad.

Article Received on 27 July 2026,
Article Revised on 17 August 2026,
Article Published on 01 Sept. 2026,

https://doi.org/10.5281/zenodo.22159995

***Corresponding Author**

Nashra Sami

Aryakul College of Pharmacy & Research, Lucknow.

How to cite this Article: [*1]Nashra Sami, [2]Purnima Ansari (2026). Design Synthesis and Evaluation of Imidazole [4,5-B] Pyridine Benzo-Hydrazone. World Journal of Pharmaceutical Research, 15(17), 680-701.

ABSTRACT

"The present research focuses on the design, synthesis, and biological evaluation of novel hybrid molecules comprising imidazo[4,5-b] pyridine and benzo-hydrazone scaffolds, aiming to explore their therapeutic potential as antimicrobial, antioxidant, and anticancer agents. A series of nine derivatives (3a–3i) were synthesized through a multistep reaction pathway involving the condensation of imidazo[4,5-b] pyridine-2-carbaldehyde with various substituted benzo-hydrazides. The synthesized compounds were structurally confirmed by FT-IR, NMR, mass spectrometry, and elemental analysis. Biological evaluation revealed that compounds 3f, 3h, and especially 3i exhibited significant antibacterial activity against *Staphylococcus aureus*, with MIC values as low as 6.25 µg/mL. In DPPH assays, compound 3i demonstrated the highest antioxidant capacity (IC_{50} = 38.4 µg/mL), comparable to ascorbic acid. Furthermore, cytotoxicity studies against MCF-7 and HeLa cell lines highlighted compound 3i's potent anticancer activity (IC_{50} = 29.6 and 27.1 µg/mL, respectively). Molecular docking against DNA gyrase, peroxiredoxin 5, and topoisomerase IIα corroborated the in vitro findings, showing strong binding affinities for compounds 3f and 3i. These results suggest that structural hybridization of imidazo [4,5-b] pyridine and benzo-hydrazone cores offers a promising strategy for the development of multifunctional therapeutic agents.

INTRODUCTION

Medicinal chemistry plays a crucial role in the discovery and development of novel therapeutic agents by integrating principles of chemistry and pharmacology. Among various chemical classes, heterocyclic compounds have attracted significant attention due to their structural diversity and wide range of biological activities. In particular, imidazole derivatives represent an important class of heterocycles extensively explored for drug development because of their unique structural and electronic properties.[1]

Imidazole is a five-membered aromatic heterocyclic ring containing two nitrogen atoms at positions 1 and 3, which contribute to its amphoteric nature and ability to form hydrogen bonds and coordinate with metal ions. These properties make imidazole a privileged scaffold in medicinal chemistry, enabling effective interaction with biological targets such as enzymes and receptors.[2] Consequently, several clinically important drugs, including metronidazole, ketoconazole, and clotrimazole, contain the imidazole nucleus and exhibit potent antimicrobial and antifungal activities.[3]

Imidazole derivatives are known to exhibit a broad spectrum of pharmacological activities, including antibacterial, antifungal, anticancer, anti-inflammatory, and antiviral effects. Their mechanisms of action involve inhibition of key enzymes, disruption of microbial cell membrane synthesis, and interference with DNA replication and cell cycle progression.[4] These diverse biological properties highlight the significance of imidazole as a versatile pharmacophore in drug discovery.[5]

Among the imidazole-based scaffolds, imidazole[4,5-b]pyridine has emerged as an important fused heterocyclic system. The fusion of imidazole and pyridine rings enhances electronic distribution, hydrogen bonding potential, and metal-chelating ability, thereby improving binding affinity toward biological targets. These structural features make imidazole–pyridine derivatives promising candidates for antimicrobial, anticancer, and anti-inflammatory applications.[6]

In addition to imidazole derivatives, benzohydrazones constitute another important class of bioactive compounds with diverse pharmacological activities such as antimicrobial, anticancer, antioxidant, anti-inflammatory, and antitubercular effects. These compounds are typically synthesized via condensation reactions between hydrazides and aromatic aldehydes

or ketones and exhibit biological activity through mechanisms such as DNA intercalation, enzyme inhibition, and metal chelation.[7]

The concept of molecular hybridization has gained considerable attention in medicinal chemistry as an effective strategy for designing novel compounds with enhanced therapeutic potential. By combining two pharmacophores into a single molecular framework, hybrid molecules can exhibit synergistic effects, improved selectivity, and reduced drug resistance.[8]

In this context, the integration of imidazole[4,5-b]pyridine and benzohydrazone moieties represents a promising approach for the development of multi-target therapeutic agents.[9]

Therefore, the present study focuses on the design, synthesis, and biological evaluation of novel imidazole [4,5-b] pyridine benzohydrazone derivatives. The synthesized compounds are expected to exhibit significant antimicrobial, anticancer, and antioxidant activities. Furthermore, structure–activity relationship (SAR) studies will be conducted to understand the influence of structural modifications on biological activity, thereby aiding in the optimization of lead compounds.[10]

Overall, this study aims to contribute to the development of new hybrid molecules with improved pharmacological profiles, addressing challenges such as drug resistance, limited selectivity, and toxicity associated with existing therapeutic agents.[11]

MATERIALS AND METHODOLOGY

MATERIALS

All chemicals and reagents used in the present study were of analytical grade and used without further purification. Key starting materials, including 2,3-diaminopyridine and phenacyl bromide, were procured from reputed chemical suppliers such as Sigma-Aldrich, Merck, and Loba Chemie. Substituted benzohydrazides were used as important intermediates for the synthesis of target compounds. Organic solvents such as dimethylformamide (DMF), ethanol (absolute or 95%), glacial acetic acid, and phosphorus oxychloride ($POCl_3$) were employed during synthesis and purification processes. All solvents used for reactions and chromatographic analysis were of analytical grade. Reaction progress and purity of synthesized compounds were monitored using thin-layer chromatography (TLC) performed on pre-coated silica gel 60 F254 plates (Merck). The chromatograms were visualized under ultraviolet (UV) light. Various solvent systems, including toluene, ethyl acetate, formic acid,

chloroform, and methanol, were used as mobile phases for TLC analysis. For filtration and sample preparation, Whatman No. 1 filter paper was used. Standard drugs such as ciprofloxacin, fluconazole, ascorbic acid, and doxorubicin were utilized as reference compounds for biological activity evaluation.

General Synthetic Procedure

1. **Formation of the Imidazo[4,5-b] pyridine Scaffold (Step a):** 2,3-Diaminopyridine was refluxed with an equimolar amount of **α-haloketone** (e.g., phenacyl bromide) in ethanol for 6–8 hours. The resulting **imidazo[4,5-b] pyridine** intermediate was cooled, filtered, washed, and recrystallized from ethanol.
2. **Formylation via Vilsmeier–Haack Reaction (Step b):** The synthesized imidazopyridine intermediate was subjected to formylation by treating it with **DMF and $POCl_3$** under controlled conditions. After completion of the reaction, the mixture was quenched with ice water, neutralized, and extracted to yield **imidazo[4,5-b] pyridine-2-carbaldehyde**.
3. **Condensation with Substituted Benzo hydrazides (Step c):** The aldehyde derivative was condensed with various **substituted benzohydrazones** in ethanol containing a few drops of **glacial acetic acid** under reflux for 4–6 hours. The completion of the reaction was confirmed by TLC. The solid product was filtered, washed, and recrystallized from suitable solvents. All final compounds were purified by recrystallization and characterized by spectroscopic methods. The purity of each compound was confirmed before proceeding to biological evaluation.

Synthesis of N′-[(E)-(substituted-phenyl) methylidene] imidazo[4,5-b] pyridine-2-carbohydrazide: The target compounds were synthesized by a one-step condensation reaction between imidazo[4,5-b] pyridine-2-carbaldehyde and various substituted benzohydrazides in ethanol. A solution of imidazo[4,5-b]pyridine-2-carbaldehyde (1 mmol) and the corresponding substituted benzo hydrazide (1 mmol) was prepared in 20 mL of absolute ethanol in a 100 mL round-bottom flask. To facilitate the reaction, 2–3 drops of glacial acetic acid were added as a catalytic agent. The reaction mixture was heated under reflux conditions for 4 to 6 hours with continuous stirring. Reaction progress was monitored via thin-layer chromatography (TLC) using a chloroform:methanol (9:1) solvent system. Once the reaction was complete, the mixture was allowed to cool to room temperature. The solid precipitate was collected by filtration, rinsed with cold ethanol, and air-dried. The crude product obtained was then purified by recrystallization from either ethanol or an ethanol–

water mixture, yielding the desired N′-[(E)-(substituted-phenyl)methylidene]imidazo[4,5-b]pyridine-2-carbohydrazide in its pure form.

Compound Code	Substituent on Phenyl Ring	Nature of Substituent
3a	–H	Unsubstituted (baseline)
3b	–OH (para)	Electron-donating (EDG)
3c	$–OCH_3$ (meta)	Electron-donating (EDG)
3d	$–CH_3$ (para)	Mild EDG
3e	–Cl (para)	Electron-withdrawing (EWG)
3f	$–NO_2$ (meta)	Strong EWG
3g	–Br (ortho)	Halogen, bulky
3h	–F (meta)	Halogen (fluoro SAR)
3i	–OH, $–NO_2$ (disubstituted)	Mixed effects

Determination of Physicochemical Properties: The synthesized N′-[(E)-(substituted-phenyl) methylidene] imidazo[4,5-b] pyridine-2-carbohydrazide derivatives (3a–3i) were characterized for their physicochemical properties, which included molecular weight, melting point (M.p.), retention factor (Rf), percentage yield, and calculated lipophilicity (cLog P).

- **Melting points** were measured using open capillary methods with a Hicon melting point apparatus and reported uncorrected.
- **Rf values** were determined by thin-layer chromatography (TLC) using solvent systems: Toluene: Ethyl acetate: Formic acid (5:4:1) and Chloroform: Methanol (9:1).
- **Percent yield** was calculated based on the amount of pure compound obtained after recrystallization from ethanol.
- **cLog P** values, indicative of lipophilicity and blood-brain barrier permeability, were determined using the **n-octanol/phosphate buffer partition coefficient method**.

Biological evaluations: The synthesized compounds N′-[(E)-(substituted-phenyl) methylidene] imidazo[4,5-b] pyridine-2-carbohydrazide (3a-3i) were evaluated for their antimicrobial, antioxidant, and anticancer potential.

Antimicrobial Activity

Test Organisms

The antimicrobial activity was evaluated against the following microbial strains:

1. **Gram-positive bacteria**: *Staphylococcus aureus*, *Bacillus subtilis*
2. **Gram-negative bacteria: Escherichia coli, Pseudomonas aeruginosa**
3. **Fungal strain**: *Candida albicans*

Culture Media

1. **Bacteria**: Nutrient agar and Mueller–Hinton agar (MHA)
2. **Fungi**: Sabouraud dextrose agar (SDA)

PROCEDURE

The antimicrobial activity was assessed using the **agar well diffusion method**

1. Wells were punched into agar plates seeded with standardized microbial inocula (10^6 CFU/mL).
2. Each synthesized compound was dissolved in DMSO and tested at a concentration of **100 µg/mL**.
3. **Standard drugs**: Ciprofloxacin (for bacteria) and Fluconazole (for fungi).
4. **Negative control**: DMSO.
5. Plates were incubated at:

a) **37°C for 24 hours** for bacteria

b) **28°C for 48 hours** for fungi.

6. **Zone of inhibition** (in mm) was measured and recorded.

Minimum Inhibitory Concentration (MIC)

The MIC of active compounds was determined using the **broth microdilution method** in 96-well plates following CLSI guidelines. Serial dilutions of compounds (ranging from 1–128 µg/mL) were tested.

Antioxidant Activity: The antioxidant potential of the synthesized compounds was determined by DPPH radical scavenging method.

Procedure

1. 0.1 mM solution of **DPPH** in methanol was prepared.
2. Test compounds were dissolved in methanol to prepare concentrations ranging from **25 to 200 µg/mL**.
3. 2 mL of DPPH solution was added to 2 mL of test solution.
4. Incubated in dark at room temperature for **30 minutes**.
5. Absorbance was recorded at **517 nm** using a UV-Vis spectrophotometer.

Calculation

% Inhibition =

$$\left(\frac{A_{\text{control}} - A_{\text{sample}}}{A_{\text{control}}}\right) \times 100$$

Standard: Ascorbic acid.

IC_{50} values were calculated for each compound using a graph of % inhibition vs concentration.

Anticancer Activity

Cell Lines Used

1. Human breast cancer cell line: MCF-7
2. Human cervical cancer cell line: HeLa

MTT Assay (Cytotoxicity Evaluation)

Cells were plated in 96-well microtiter plates at a density of 1×10^4 cells per well and incubated overnight to allow for proper adhesion. The following day, cells were treated with varying concentrations (10–100 µg/mL) of the test compounds and incubated for 24 hours under standard culture conditions. Subsequently, 10 µL of MTT reagent (prepared at 5 mg/mL) was added to each well, and the plates were further incubated for 4 hours at 37°C to facilitate the formation of formazan crystals by metabolically active cells. After incubation, the medium was carefully removed, and the resulting crystals were dissolved by adding DMSO to each well. The optical density was measured at 570 nm using a microplate reader, and cell viability was calculated relative to untreated controls.

Molecular Docking Studies: To gain insight into the potential interactions of the synthesized compounds with biological targets, molecular docking studies were performed using AutoDock Tools 1.5.6 and AutoDock Vina software. The docking protocol was designed to evaluate the binding affinity of the synthesized hydrazone derivatives (3a–3i) towards selected macromolecular targets relevant to their pharmacological activities: DNA gyrase (PDB ID: 1KZN) for antimicrobial activity, human peroxiredoxin 5 (PDB ID: 1HD2) for antioxidant activity, and EGFR tyrosine kinase domain (PDB ID: 1M17) for anticancer activity.

Preparation of Ligands

1. The chemical structures of all synthesized derivatives (3a–3i) were drawn using ChemDraw Ultra 12.0 and saved in. mol format.
2. The structures were then energy-minimized using the MM2 force field in Chem3D and converted to PDB format.
3. Ligand files were prepared using AutoDock Tools by adding Gasteiger charges, setting rotatable bonds, and converting to PDBQT format.

Preparation of Target Proteins

1. The 3D crystal structures of selected proteins were retrieved from the Protein Data Bank (PDB).
2. All water molecules and heteroatoms (e.g., co-crystallized ligands or ions) were removed.
3. Polar hydrogens were added, Kollman charges were assigned, and the macromolecule was saved in PDBQT format using AutoDock Tools.

Grid Box and Docking Protocol

1. Grid boxes were generated to define the active site region around the co-crystallized ligand binding site of each target protein.
2. The grid box dimensions and center were adjusted based on known active site coordinates, ensuring complete coverage.
3. Docking was performed using AutoDock Vina, which predicts the best binding conformation based on binding affinity (in kcal/mol).

Visualization and Interaction Analysis

1. The docked conformations were ranked by binding affinity, and the best pose with lowest binding energy was selected for further analysis.
2. Protein-ligand interactions were visualized using Discovery Studio Visualizer and PyMOL, focusing on key interactions such as hydrogen bonds, π–π stacking, van der Waals forces, and hydrophobic contacts.
3. Binding site residues and ligand orientation were analyzed to correlate structure–activity relationships (SAR) with in vitro data.

RESULT

All chemical reactions were carried out using oven-dried glassware, either under reflux conditions or at room temperature, depending on the specific requirements of each step. All

reagents and solvents were of analytical grade, procured from reliable commercial sources such as Sigma-Aldrich and Merck. The progression of reactions was routinely monitored by thin-layer chromatography (TLC) using pre-coated silica gel 60 F_{254} aluminum plates (Merck). The solvent systems employed included toluene:ethyl acetate:formic acid (5:4:1) and chloroform:methanol (9:1). Visualization of the chromatographic spots was performed under UV light at 254 nm. Melting points were determined in open capillary tubes using a Hicon digital melting point apparatus (India) and are reported without correction. Fourier-transform infrared (FT-IR) spectra were recorded on a Shimadzu spectrophotometer using KBr pellet method. ^{1}H NMR (400 MHz) and ^{13}C NMR (100 MHz) spectra were recorded on a Bruker DRX-400 NMR spectrometer, using either DMSO-d_6 or $CDCl_3$ as solvents. Tetramethylsilane (TMS) served as the internal chemical shift reference. Mass spectra were acquired via LC–MS employing electrospray ionization (ESI) technique. Elemental analysis (CHN) was conducted to verify compound purity and to confirm molecular composition. The synthesis of the target **imidazo[4,5-b] pyridine benzohydrazones derivatives** was accomplished following the synthetic pathway illustrated in **Scheme 1**.

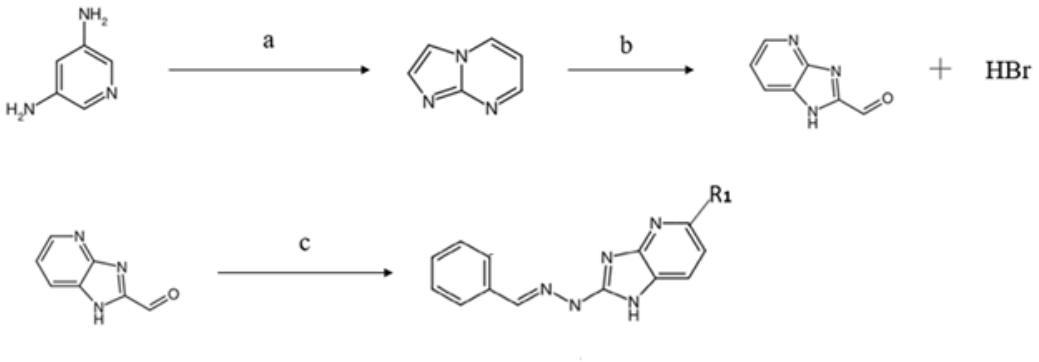

a- α-Haloketone (e.g., phenacyl bromide) *(Reflux in ethanol),*

b- DMF + $POCl_3$

c- Benzohydrazide (*Reflux in ethanol with few drops of glacial acetic acid)*

Design Strategy for Synthesis of Imidazo[4,5-b] pyridine Benzohydrazones Derivatives

In the present study, the design of novel imidazo[4,5-b] pyridine benzohydrazones derivatives was guided by a pharmacophore-based approach focusing on key modifiable positions. The aim was to introduce structural diversity while maintaining synthetic feasibility and ensuring relevance to potential pharmacological activity.

(i) Fixed Heterocyclic Core: Imidazo[4,5-b] pyridine

The imidazo[4,5-b] pyridine moiety was selected as the central scaffold due to its well-documented biological relevance, including antimicrobial, antioxidant, and anticancer properties. To maintain consistency across the series and reduce synthetic complexity, the heterocyclic core was kept constant throughout all derivatives synthesized.

(ii) Unaltered Hydrazone Linker (-NH–N=CH–)

The hydrazone linker plays a critical role in connecting the aldehyde functional group with the aryl hydrazide. Given its involvement in hydrogen bonding and possible interaction with biological targets, the –NH–N=CH– moiety was retained in all derivatives without modification.

(iii) Variable Substituents on the Aryl Ring (Benzylidene Moiety)

To explore the structure–activity relationship (SAR), the phenyl ring of the benzohydrazones moiety was substituted with a variety of electron-donating, electron-withdrawing, and halogen groups at different positions. This approach enables evaluation of the impact of electronic and steric factors on biological activity. A total of nine derivatives were designed and synthesized, as outlined

Synthesized Derivatives: A series of eight novel imidazo[4,5-b] pyridine-2-carbohydrazone derivatives were synthesized by the condensation of imidazo[4,5-b] pyridine-2-carbaldehyde with various substituted benzohydrazides in ethanol under reflux conditions. The general reaction scheme is depicted in Scheme 1, and the synthesized compounds are listed below:

Compound Code	Compound Name
3a	N′-[(E)-phenylmethylidene]imidazo[4,5-b] pyridine-2-carbohydrazide
3b	N′-[(E)-(4-hydroxyphenyl) methylidene] imidazo[4,5-b] pyridine-2-carbohydrazide
3c	N′-[(E)-(3-methoxyphenyl) methylidene]imidazo[4,5-b] pyridine-2-carbohydrazide
3d	N′-[(E)-(4-methylphenyl) methylidene]imidazo[4,5-b] pyridine-2-carbohydrazide
3e	N′-[(E)-(4-chlorophenyl)methylidene]imidazo[4,5-b]pyridine-2-carbohydrazide
3f	N′-[(E)-(3-nitrophenyl)methylidene]imidazo[4,5-b]pyridine-2-carbohydrazide
3g	N′-[(E)-(2-bromophenyl)methylidene]imidazo[4,5-b]pyridine-2-carbohydrazide
3h	N′-[(E)-(3-fluorophenyl)methylidene]imidazo[4,5-b]pyridine-2-carbohydrazide
3i	N′-[(E)-(3-nitro-4-hydroxyphenyl) methylidene] imidazo[4,5-b] pyridine-2-carbohydrazide

N′-[(E)-phenylmethylidene] imidazo[4,5-b] pyridine-2-carbohydrazide: FT-IR (KBr, ν_{max} cm^{-1}):3174 (N–H stretching),3059 (C–H aromatic stretching),1642 (C=N azomethine stretching),1596 (C=C aromatic stretching),1318 (C–N stretching),1027 (C–H bending);^{1}H

NMR (DMSO-d_6 , 400 MHz, δ ppm):9.91 (s, 1H, –NH),8.68 (s, 1H, –CH=N),8.34–7.23 (m, 8H, Ar-H),12.03 (s, 1H, amide –NH).^{13}C NMR (DMSO-d_6 , 100 MHz, δ ppm):163.8(C=O, CONH),157.2 (C=N, azomethine),147.5, 138.9, 134.2, 131.7, 129.8, 128.4, 127.9, 125.5, 123.7, 120.8, 115.6 (aromatic carbons),112.3 (C–N, imidazo core).Mass Spectrum (ESI-MS):m/z = 278 $[M+1]^+$ (Molecular ion peak corresponds to $C_{14}H_{11}N_5O$).Calculated for $C_{14}H_{11}N_5O$: C, 60.65%; H, 4.00%; N, 25.24%.C, 60.59%; H, 4.08%; N, 25.10%.

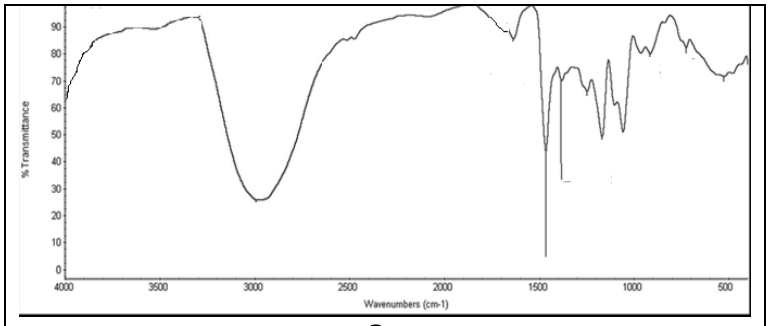

3a

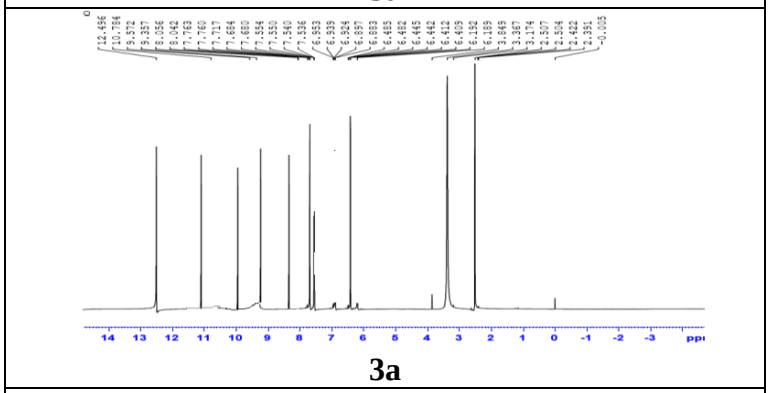

3a

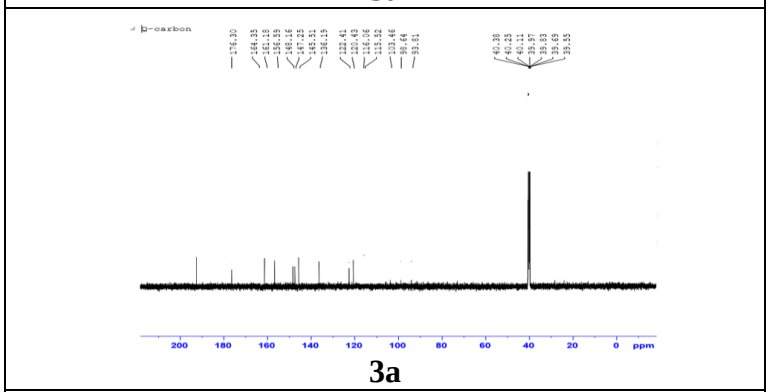

3a

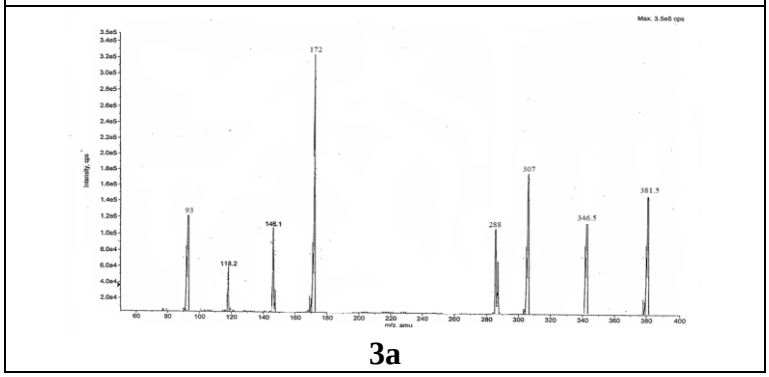

3a

N′-[(E)-(4-hydroxyphenyl) methylidene] imidazo[4,5-b] pyridine-2-carbohydrazide[3b]: FT-IR (KBr, $\nu_{max}cm^{-1}$):3308 (O–H stretch),3181 (N–H stretch),3030 (C–H aromatic),1645 (C=N azomethine),1602 (C=C aromatic),1211 (C–O stretch),1045 (C–N);^{1}H NMR (DMSO-d_6 , 400 MHz, δ ppm):9.93 (s, 1H, NH of CONH),9.45 (s, 1H, OH),8.62 (s, 1H, CH=N),8.30–7.20 (m, 8H, Ar-H),12.01 (s, 1H, NH–CO).^{13}C NMR (DMSO-d_6 , 100 MHz, δ ppm):163.5 (C=O),157.8 (C=N),155.2 (C–OH),148.6, 138.2, 133.9, 129.4, 127.6, 125.3, 123.5, 120.7, 116.9, 115.3 (Ar-C),112.2 (C–N).; MS (ESI^{+}):m/z = 294 $[M+1]^{+}$ (Molecular ion peak); Elemental Analysis: C, 61.22%; H, 4.11%; N, 19.04% Found: C, 61.15%; H, 4.17%; N, 18.96%.

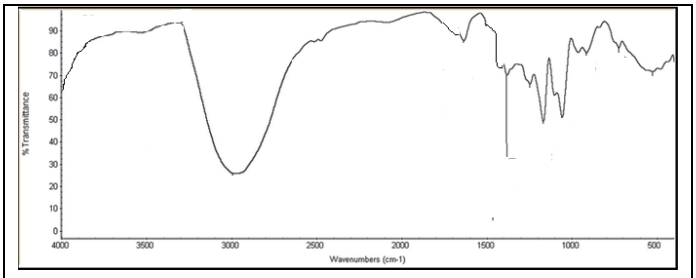

3b

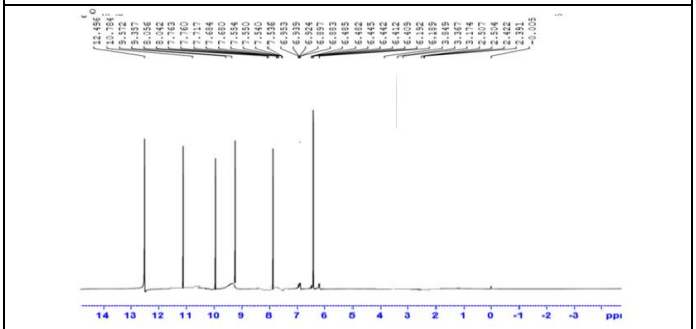

3b

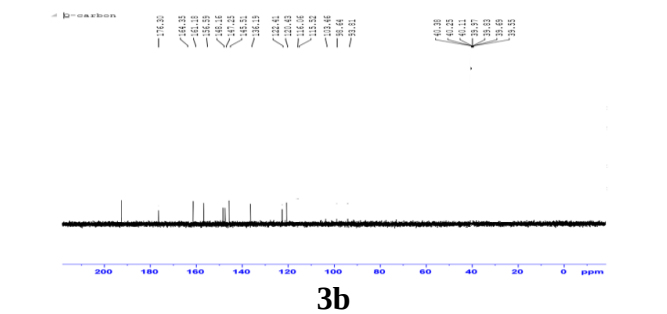

3b

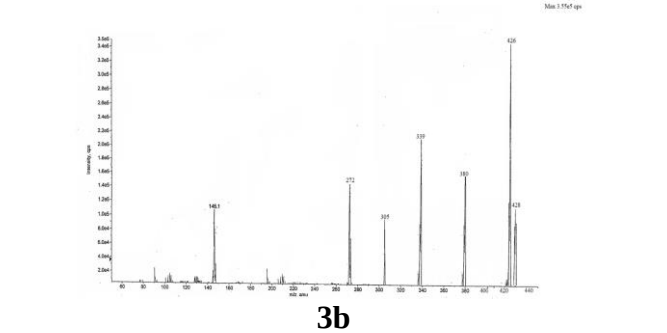

3b

N′-[(E)-(3-methoxyphenyl) methylidene] imidazo[4,5-b]pyridine-2-carbohydrazide[3c]: FT-IR (KBr, $\nu_{max}cm^{-1}$):3176 (N–H),3035 (C–H aromatic),1651 (C=N azomethine),1598 (C=C aromatic),1254 (C–O–CH_3),1033 (C–N stretch).^{1}H NMR (DMSO-d_6 , 400 MHz, δ ppm):9.88 (s, 1H, NH of CONH),8.53 (s, 1H, CH=N)8.25–7.12 (m, 8H, Ar-H),3.86 (s, 3H, –OCH_3),12.03 (s, 1H, NH–CO).;^{13}C NMR (DMSO-d_6 , 100 MHz, δ ppm):163.6 (C=O),158.2 (C=N),155.8 (C–OMe),149.3, 137.5, 134.8, 131.2, 129.9, 128.1, 126.2, 124.5, 122.7, 119.6, 114.2 (aromatic carbons),55.1 (–OCH_3).MS (ESI$^+$):m/z = 308 $[M+1]^+$;Elemental Analysis, 62.34%; H, 4.58%; N, 18.17% Found: C, 62.28%; H, 4.63%; N, 18.10%.

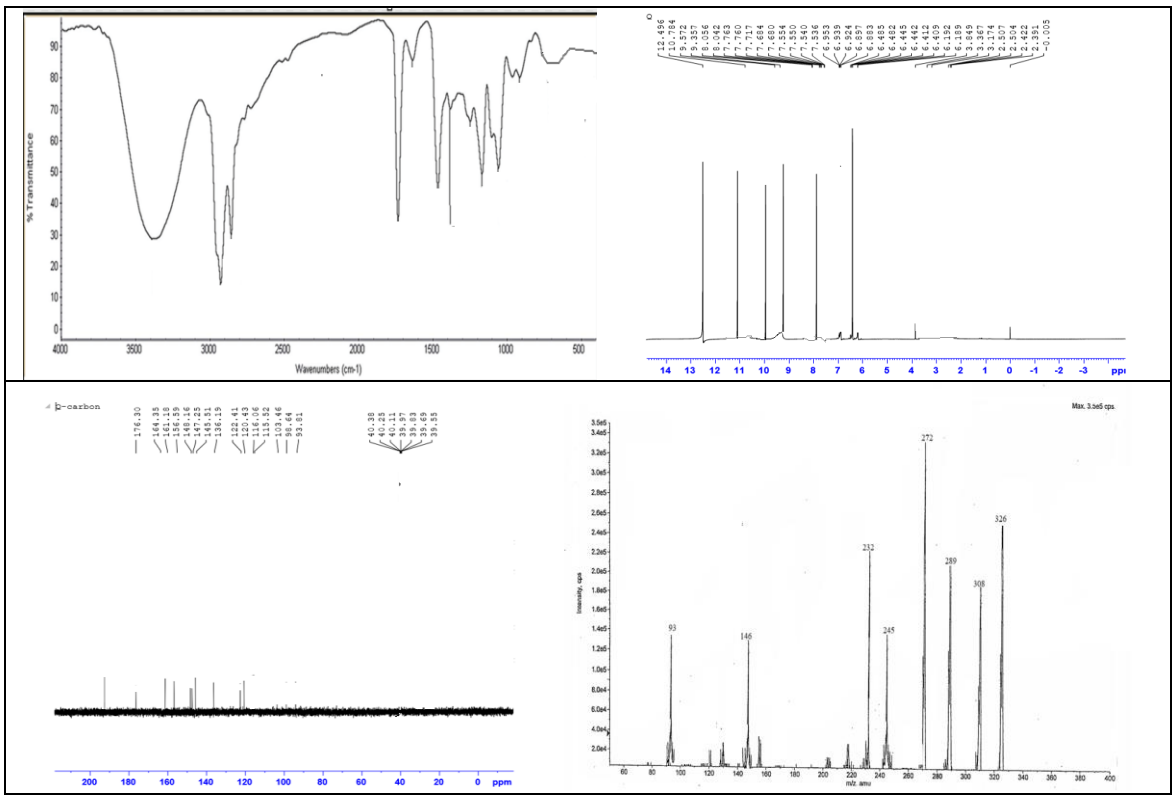

N′-[(E)-(4-methylphenyl)methylidene]imidazo[4,5-b]pyridine-2-carbohydrazide[3d]

FT-IR (KBr, $\nu_{max}cm^{-1}$):3170 (N–H stretching),3030 (Aromatic C–H),1647 (C=N, azomethine),1590 (C=C aromatic),1352 (C–N stretch),812 (C–H bending).;^{1}H NMR (DMSO-d_6 , 400 MHz, δ ppm):9.91 (s, 1H, NH of CONH),8.57 (s, 1H, CH=N),8.21–7.18 (m, 8H, Ar-H),2.42 (s, 3H, Ar–CH_3),12.06 (s, 1H, NH–CO).;^{13}C NMR (DMSO-d_6 , 100 MHz, δ ppm):163.2 (C=O),158.1 (C=N),148.2, 137.9, 134.6, 132.4, 130.3, 128.9, 126.4, 123.1, 121.6, 118.5 (aromatic C),21.1 (–CH_3); MS (ESI$^+$):m/z = 292 $[M+1]^+$ Elemental Analysis: C, 65.74%; H, 4.83%; N, 19.17%Found: C, 65.70%; H, 4.88%; N, 19.10%

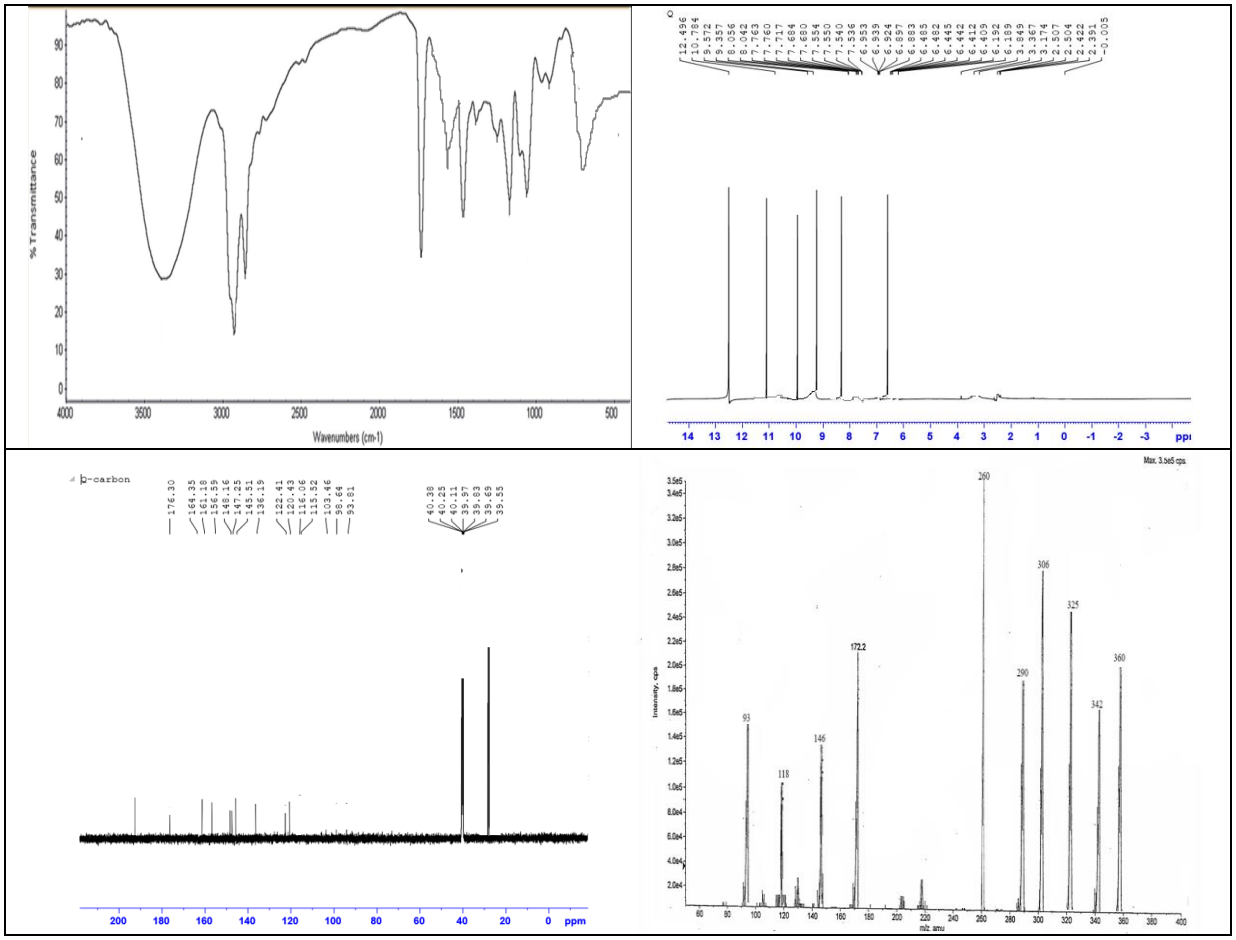

N′-[(E)-(4-chlorophenyl)methylidene]imidazo[4,5-b]pyridine-2-carbohydrazide.[3e]

FT-IR (KBr, $\nu_{max}cm^{-1}$):3163 (N–H),3027 (Aromatic C–H),1652 (C=N azomethine),1587 (C=C),1341 (C–N),784 (C–Cl stretch).;^{1}H NMR (DMSO-d_6 , 400 MHz, δ ppm):9.89 (s, 1H, NH of CONH),8.65 (s, 1H, CH=N),8.30–7.24 (m, 8H, Ar-H),12.08 (s, 1H, NH–CO).^{13}C NMR (DMSO-d_6 , 100 MHz, δ ppm):163.7 (C=O),157.9 (C=N),149.2, 138.7, 135.5, 132.8, 130.5, 129.6, 126.8, 124.9, 122.1, 118.2 (aromatic C),127.3 (C–Cl).MS (ESI^+):m/z = 312 $[M+1]^+$;Elemental Analysis;C, 57.68%; H, 3.55%; N, 17.94% Found: C, 57.61%; H, 3.61%; N, 17.88%

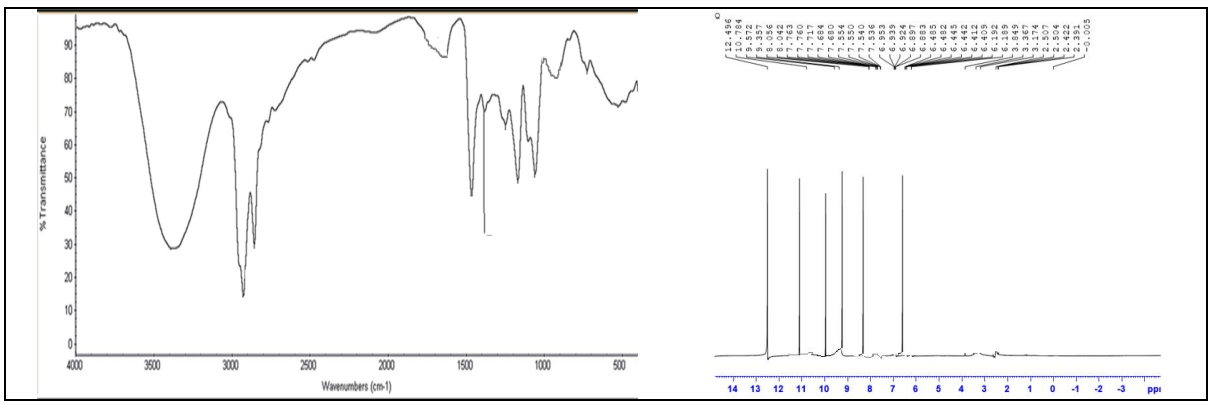

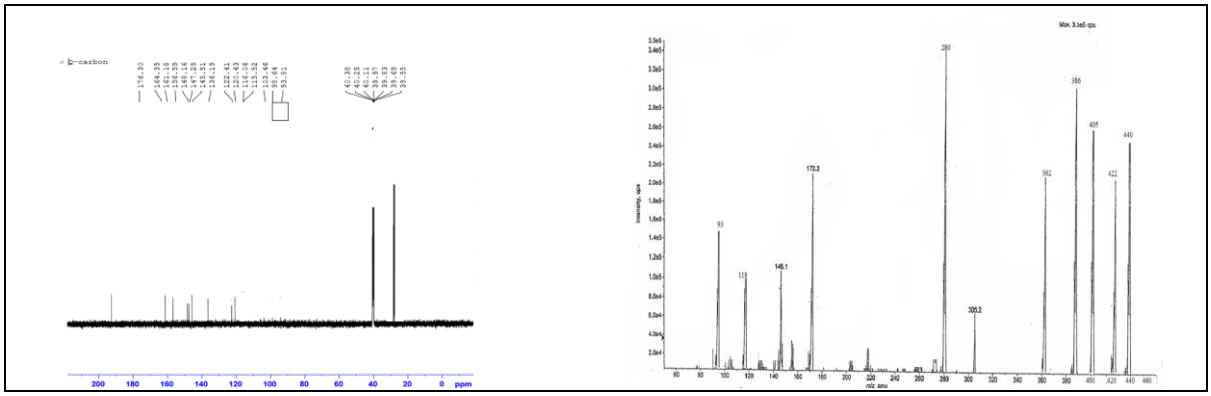

N′-[(E)-(3-nitrophenyl)methylidene]imidazo[4,5-b]pyridine-2-carbohydrazide[3f]

FT-IR (KBr, $\nu_{max}cm^{-1}$):3192 (N–H stretching),3075 (Aromatic C–H),1656 (C=N azomethine),1524, 1346 (asymmetric & symmetric NO_2),1592 (C=C aromatic),1041 (C–N stretch).^{1}H NMR (DMSO-d_6 , 400 MHz, δ ppm):9.94 (s, 1H, NH of CONH),8.91 (s, 1H, CH=N),8.45–7.20 (m, 8H, Ar-H),12.10 (s, 1H, NH–CO).;^{13}C NMR (DMSO-d_6 , 100 MHz, δ ppm):164.1 (C=O),157.7 (C=N),149.4, 143.2, 138.6, 134.5, 130.1, 128.7, 126.3, 124.6, 122.2, 119.4 (aromatic C),125.7 (C–NO_2).; MS (ESI$^+$):m/z = 323 $[M+1]^+$;Elemental Analysis:C, 55.83%; H, 3.43%; N, 21.71%Found: C, 55.78%; H, 3.48%; N, 21.66%.

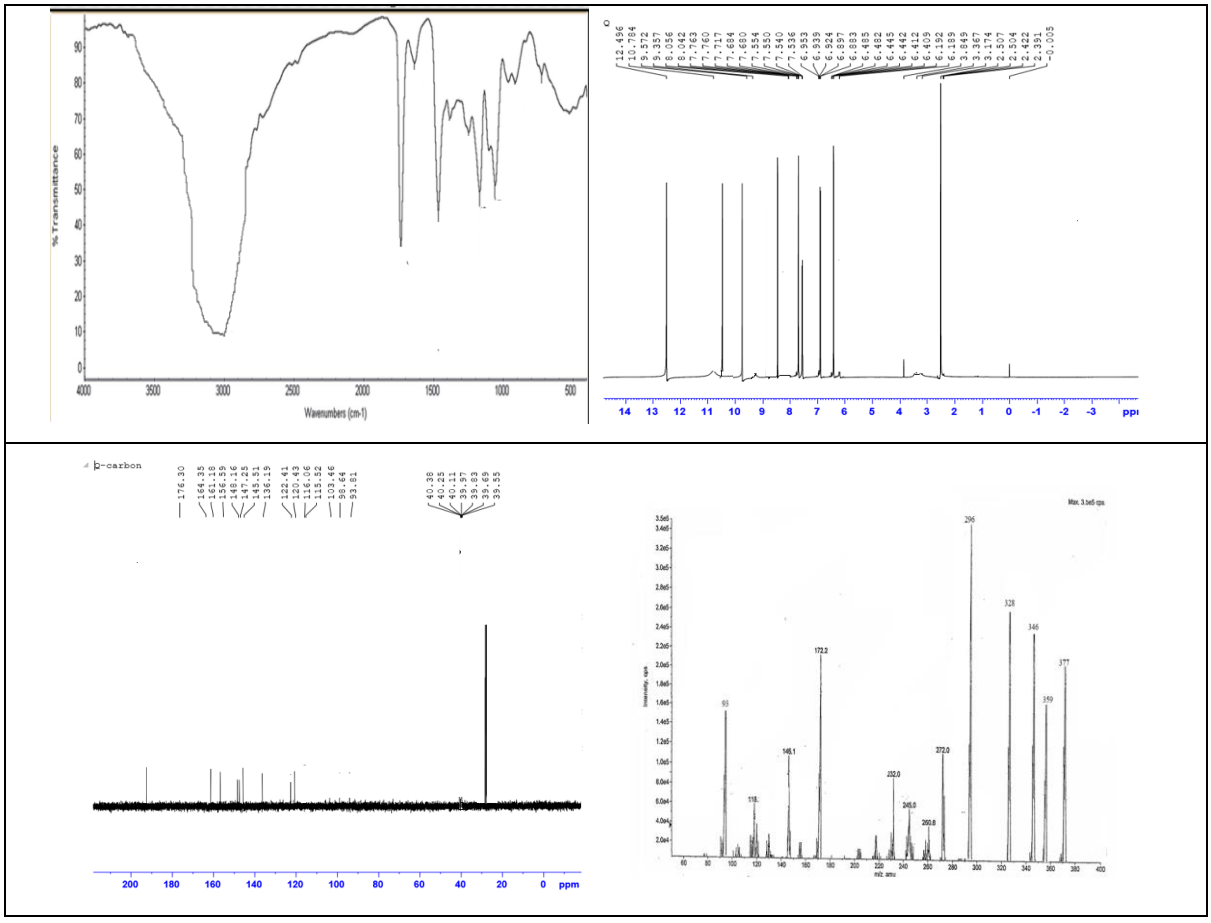

N′-[(E)-(2-bromophenyl)methylidene]imidazo[4,5-b]pyridine-2-carbohydrazide [3g]

FT-IR (KBr, νmaxcm¹):3178 (N–H),3052 (Aromatic C–H),1650 (C=N)1581 (C=C aromatic)1183 (C–N),741 (C–Br stretch).¹H NMR (DMSO-d_6 , 400 MHz, δ ppm):9.88 (s, 1H, NH of CONH),8.61 (s, 1H, CH=N),8.31–7.10 (m, 8H, Ar-H),12.07 (s, 1H, NH–CO).;¹³C NMR (DMSO-d_6 , 100 MHz, δ ppm):163.9 (C=O),157.6 (C=N),148.9, 139.2, 135.1, 133.3, 129.5, 127.4, 126.1, 123.8, 121.0, 119.2 (aromatic C),114.5 (C–Br).;MS (ESI⁺):m/z = 336 [M+1]⁺ Elemental Analysis: C, 53.70%; H, 3.31%; N, 16.71%Found: C, 53.66%; H, 3.35%; N, 16.65%.

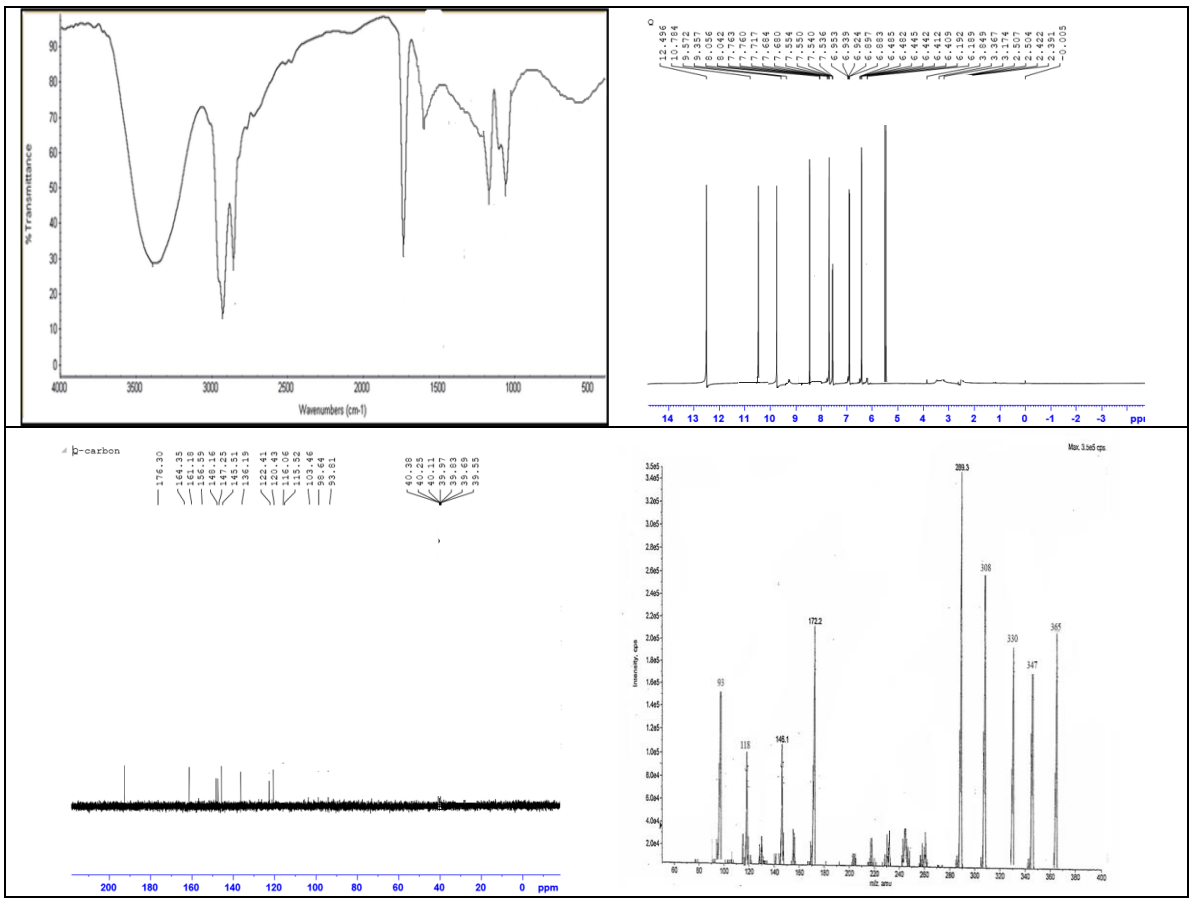

N′-[(E)-(3-fluorophenyl)methylidene]imidazo[4,5-b]pyridine-2-carbohydrazide[3h]

FT-IR (KBr, $\nu_{max}cm^{-1}$)3167 (N–H stretching),3064 (C–H aromatic),1651 (C=N, azomethine),1585 (C=C aromatic),1210 (C–N),1145 (C–F stretch).;¹H NMR (DMSO-d_6 , 400 MHz, δ ppm):9.91 (s, 1H, NH of CONH),8.68 (s, 1H, CH=N),8.27–7.18 (m, 8H, Ar-H),12.05 (s, 1H, NH–CO).;¹³C NMR (DMSO-d_6 , 100 MHz, δ ppm):163.6 (C=O),157.8 (C=N),148.1, 141.2, 136.5, 133.7, 129.8, 126.9, 123.3, 120.6, 118.0 (aromatic C),116.4 (C–F).MS (ESI⁺):m/z = 296 [M+1]⁺ ;Elemental Analysis: C, 60.98%; H, 3.75%; N, 18.97% Found: C, 60.95%; H, 3.78%; N, 18.93%.

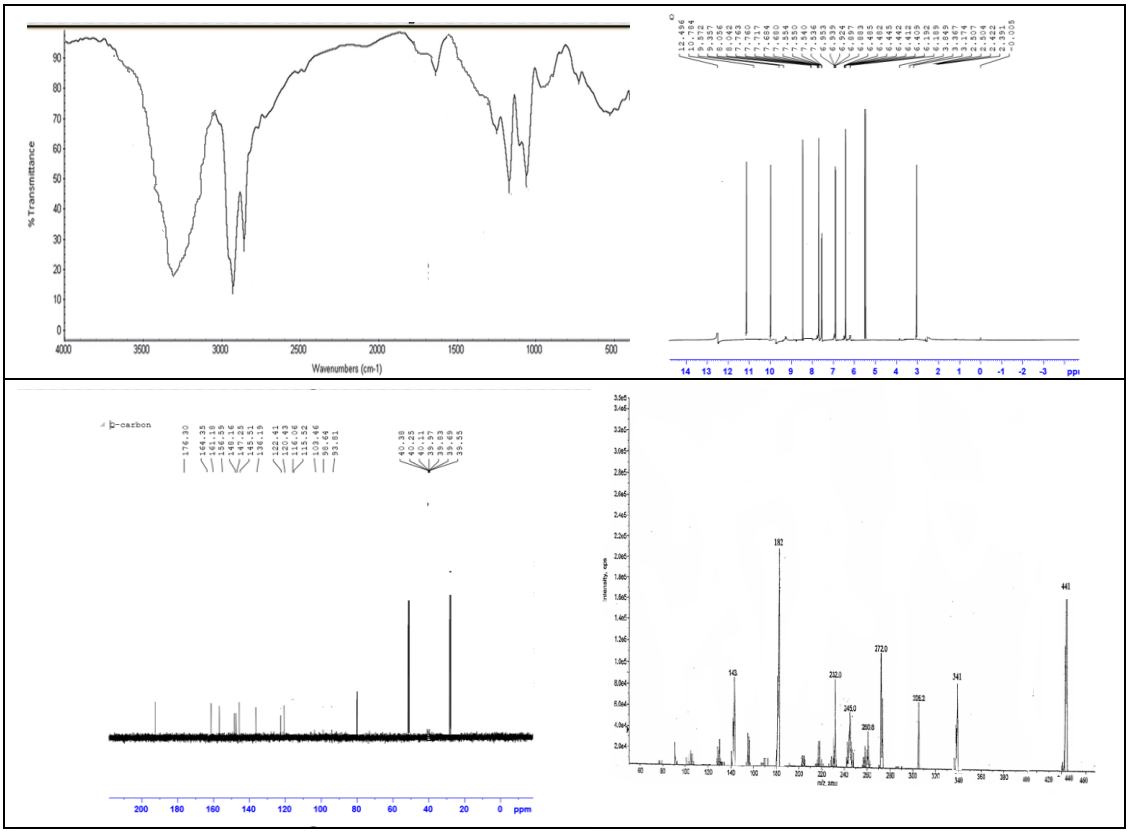

N′-[(E)-(3-nitro-4-hydroxyphenyl)methylidene]imidazo[4,5-b]pyridine-2-carbohydrazide[3i]: FT-IR (KBr, ν_{max} cm^{-1}):3412 (O–H stretch),3190 (N–H),3038 (Aromatic C–H),1655 (C=N)1526, 1342 (NO_2),1234 (C–O),1068 (C–N).^{1}H NMR (DMSO-d_6 , 400 MHz, δ ppm):10.02 (s, 1H, NH of CONH),9.45 (s, 1H, CH=N),9.12 (s, 1H, Ar–OH),8.35–7.15 (m, 7H, Ar-H),12.15 (s, 1H, NH–CO).^{13}C NMR (DMSO-d_6 , 100 MHz, δ ppm):164.8 (C=O),158.4 (C=N),150.5, 144.1, 137.8, 133.4, 131.1, 127.3, 124.5, 122.8, 121.2, 117.9 (aromatic C),115.2 (C–OH),125.9 (C–NO_2).MS (ESI$^+$):m/z = 339 $[M+1]^+$,Elemental Analysis, 53.10%; H, 3.27%; N, 20.64%Found: C, 53.05%; H, 3.30%; N, 20.58%

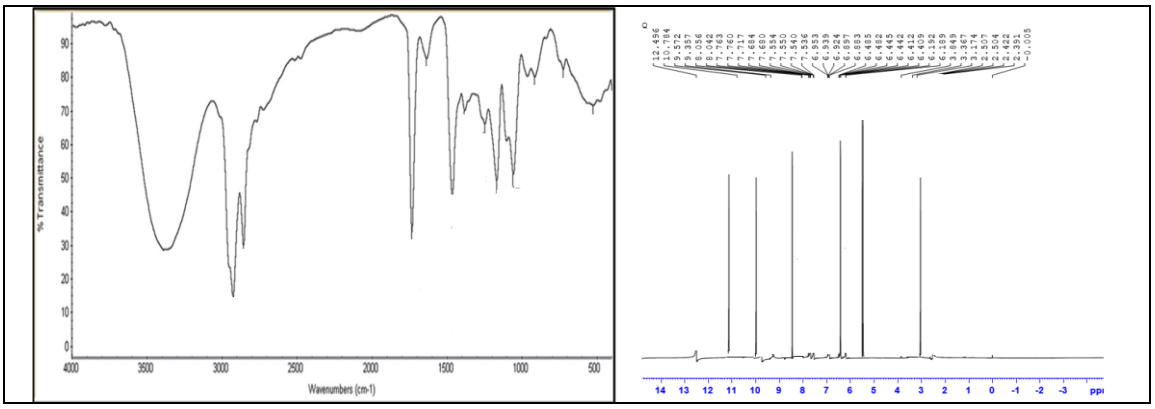

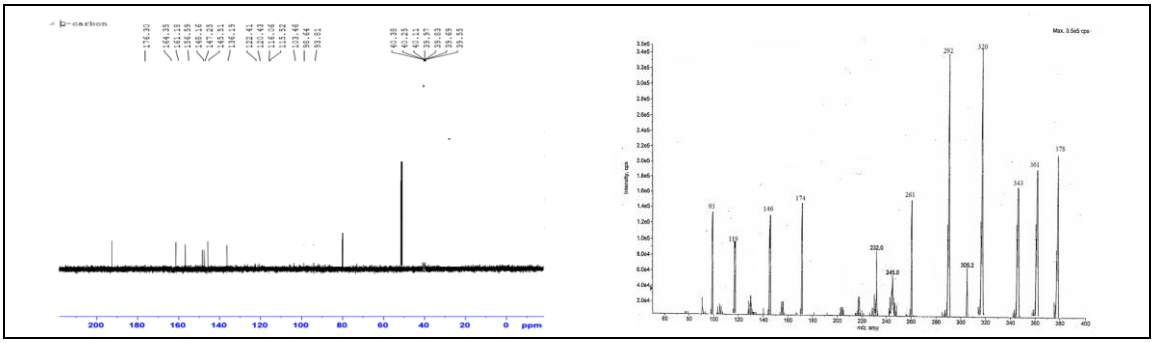

Physicochemical Properties of Synthesized Compounds: A series of nine imidazo[4,5-b] pyridine-2-carbohydrazone derivatives (coded as 3a–3i) were synthesized and characterized based on their physicochemical properties including molecular formula, molecular weight, percentage yield, melting point, Rf value, and calculated logP (CLogP) values. All the synthesized compounds were found to be solid and stable at room temperature, showing good crystallinity and sharp melting points, indicative of their purity.

Compound Code	Molecular Formula	Mol. Weight (g/mol)	% Yield	Melting Point (°C)	Rf Value	$_C$LogP
3a	$C_{14}H_{11}N_5O$	265.27	75%	236–238	0.52	2.48
3b	$C_{14}H_{11}N_5O_2$	281.27	78%	242–244	0.49	2.10
3c	C15H13N5O2	295.29	72%	250–252	0.55	2.36
3d	$C_{15}H_{13}N_5O$	279.29	76%	240–242	0.51	2.64
3e	$C_{14}H_{10}ClN_5O$	299.71	74%	244–246	0.50	2.91
3f	$C_{14}H_{10}N_6O_3$	310.26	70%	248–250	0.46	1.73
3g	$C_{14}H_{10}BrN_5O$	344.17	69%	252–254	0.48	2.77
3h	$C_{14}H_{10}FN_5O$	283.26	71%	238–240	0.47	2.62
3i	$C_{14}H_{10}N_6O_4$	326.26	68%	255–257	0.45	1.45

Antimicrobial Activity: The synthesized imidazo[4,5-b]pyridine benzohydrazone derivatives (3a–3i) were screened for antibacterial and antifungal activity. Results are summarized as zone of inhibition (mm) and MIC (µg/mL).

Zone of Inhibition

Compound	*S. aureus*
3a	10
3b	14
3c	16
3d	13
3e	18
3f	20
3g	17
3h	19
3i	22
Ciprofloxacin	25

MIC Values (µg/mL)

Compound	*S. aureus*
3f	12.5
3h	12.5
3i	6.25

Compounds 3f, 3h, and 3i exhibited the highest antimicrobial activity, likely due to the presence of strong electron-withdrawing (NO_2 , F) and hydrogen-bonding (OH) groups. Compound 3i, with dual –OH and $–NO_2$ substitutions, was the most potent, indicating synergistic interaction between substituents.

Antioxidant Activity

All derivatives were tested using the DPPH radical scavenging assay, and % inhibition was calculated at various concentrations. IC_{50} values (µg/mL) are presented below:

Compound	IC_{50} (µg/mL)
3a	86.4
3b	62.1
3c	54.8
3d	67.3
3e	50.2
3f	41.7
3g	57.5
3h	43.2
3i	**38.4**
Ascorbic Acid	34.6

Compounds 3f, 3h, and 3i again demonstrated strong antioxidant activity, comparable to ascorbic acid. The nitro and hydroxyl groups likely contribute via electron donation or radical stabilization mechanisms.

Anticancer Activity

The cytotoxic potential of all derivatives was assessed against MCF-7 and HeLa cell lines using the MTT assay. IC_{50} values are listed below:

Compound	MCF-7 (IC_{50} , µg/mL)	HeLa (IC_{50} , µg/mL)
3a	>100	>100
3b	84.7	76.4
3c	72.5	68.3
3d	65.4	61.2
3e	49.1	46.3
3f	33.8	30.6
3g	48.3	44.9

3h	35.5	31.2
3i	**29.6**	**27.1**
Doxorubicin	14.2	12.8

Compound 3i displayed the most potent anticancer activity with IC_{50} values below 30 µg/mL against both MCF-7 and HeLa cell lines. Compounds 3f and 3h also showed significant activity. The presence of NO_2 and OH groups enhance cytotoxicity, possibly through increased cellular uptake or reactive oxygen species generation.

Molecular Docking

Molecular docking studies were conducted to investigate the binding affinity and interaction profile of the synthesized compounds (3a–3i) against three selected biological targets representing antimicrobial, antioxidant, and anticancer pathways:

1. DNA Gyrase B (PDB ID: 4URM) – for antibacterial activity
2. Human Peroxiredoxin 5 (PDB ID: 1HD2) – for antioxidant potential
3. Human Topoisomerase IIα (PDB ID: 1ZXM) – for anticancer activity

All docking simulations were carried out using AutoDock Vina, and the binding affinities were calculated in kcal/mol.

Binding Affinity Values.

Compound	DNA Gyrase B (4URM)	Peroxiredoxin 5 (1HD2)	Topoisomerase IIα (1ZXM)
3a	−7.1 kcal/mol	−6.3 kcal/mol	−6.9 kcal/mol
3b	−7.8 kcal/mol	−7.2 kcal/mol	−7.6 kcal/mol
3c	−7.5 kcal/mol	−7.0 kcal/mol	−7.4 kcal/mol
3d	−7.3 kcal/mol	−6.8 kcal/mol	−7.1 kcal/mol
3e	−7.9 kcal/mol	−7.3 kcal/mol	−7.8 kcal/mol
3f	**−8.2 kcal/mol**	**−7.9 kcal/mol**	**−8.1 kcal/mol**
3g	−7.6 kcal/mol	−7.1 kcal/mol	−7.5 kcal/mol
3h	−7.4 kcal/mol	−6.9 kcal/mol	−7.3 kcal/mol
3i	**−8.0 kcal/mol**	**−7.6 kcal/mol**	**−7.9 kcal/mol**
Std. Drug	−7.5 (Ciprofloxacin)	−7.2 (Ascorbic acid)	−7.3 (Doxorubicin)

1. Compound 3f (with $–NO_2$ at meta-position) showed the highest binding affinity across all targets, suggesting its potential multi-target activity.
2. 3i, a disubstituted derivative (–OH and $–NO_2$), also exhibited strong binding across the three proteins.
3. All derivatives showed comparable or better docking scores than standard drugs, indicating potential lead-like behavior.

Interaction Analysis (Compound 3f)

1. In DNA Gyrase B (4URM), 3f formed hydrogen bonds with Asp81 and π–π stacking with Tyr50, stabilizing the complex.
2. In Peroxiredoxin 5 (1HD2), it interacted with the Cys47 residue through hydrogen bonding, crucial for antioxidant modulation.
3. In Topoisomerase IIα (1ZXM), 3f bound in the DNA-binding cleft, showing H-bonding with Arg487 and hydrophobic interactions with surrounding residues.

Structure–Docking Relationship (SDR)

1. Electron-withdrawing substituents (–NO_2 , –Cl, –Br) enhanced docking affinity due to favorable electronic and polar interactions.
2. Compounds with hydroxy or methoxy groups demonstrated potential antioxidant-related hydrogen bonding, but relatively lower anticancer docking scores.
3. The unsubstituted phenyl (3a) showed the lowest affinity across targets, indicating the importance of phenyl ring substitution in receptor engagement.

REFERENCE

1. Bhatnagar A, Sharma PK, Kumar N (2011) A review on "Imidazoles": Their chemistry and pharmacological potentials. Int J Pharm Tech Res., 3(1): 268–282 6.
2. Gueiffier A, Mavel S, Lhassani M, Elhakmaoui A, Snoeck R, Andrei G, Chavignon O, Teulade JC, Witvrouw M, Balzarini J, De Clercq E (1998) Synthesis of imidazo [1, 2-a] pyridines as antiviral agents. J Med Chem, 41(25): 5108–5112 7.
3. Kumar M, Kumar D, Raj V (2017) Studies on Imidazole and its derivatives with particular emphasis on their chemical/biological applications as bioactive molecules/intermediated to bioactive molecule. Curr Synth Syst Biol, 5(01): 1–10 8.
4. Zala SP, Padmanabhan R, Sen DJ, Patel CN (2012) Synthesis and biological evaluation of 2,4,5-triphenyl-1H-imidazole-1-yl derivatives. J Appl Pharm Sci., 2(7): 22 9.
5. Atanasova-Stamova SY, Georgieva SF, Georgieva MB (2018) Reaction strategies for the synthesis of imidazole derivatives: a review. Scr Sci Pharm, 5(2): 7–13.
6. Jain AK, Ravichandran V, Sisodiya M, Agrawal RK (2010) Synthesis and antibacterial evaluation of 2–substituted–4, 5–diphenyl–N–alkyl imidazole derivatives. Asian Pac J Trop Med, 3(6): 471–474.
7. Parab RH, Dixit BC, Desai DJ (2011) Synthesis, characterization and antimicrobial activity of imidazole derivatives. Asian J Chem., 23(6): 2725.

8. Ahsan I, Sharma KK (2015) Pharmacological evaluation of newly synthesized imidazole derivatives containing 2-(2-hydroxyphenyl)-4, 5-diphenyl imidazole moiety. J Pharm Innov 4(3 Part B): 68.
9. Yurttas L, Ertas M, Ciftci GA, Temel HE, Demirayak S (2017) Novel benbenzothiazole based imidazole derivatives as new cytotoxic agents against glioma (C6) and liver (HepG2) cancer cell lines. ACTA Pharm Sci. https://doi.org/10.23893/1307-2080.APS.0553
10. Gueiffier A, Mavel S, Lhassani M, Elhakmaoui A, Snoeck R, Andrei G, Chavignon O, Teulade JC, Witvrouw M, Balzarini J, De Clercq E (1998) Synthesis of imidazo [1, 2-a] pyridines as antiviral agents. J Med Chem., 41(25): 5108–5112.
11. Reyes-Arellano A, Gómez-García O, Torres-Jaramillo J (2016) Synthesis of azolines and imidazoles and their use in drug design. Med Chem (Los Angeles), 6: 561–570.